



저작자표시-비영리-변경금지 2.0 대한민국

이용자는 아래의 조건을 따르는 경우에 한하여 자유롭게

- 이 저작물을 복제, 배포, 전송, 전시, 공연 및 방송할 수 있습니다.

다음과 같은 조건을 따라야 합니다:



저작자표시. 귀하는 원저작자를 표시하여야 합니다.



비영리. 귀하는 이 저작물을 영리 목적으로 이용할 수 없습니다.



변경금지. 귀하는 이 저작물을 개작, 변형 또는 가공할 수 없습니다.

- 귀하는, 이 저작물의 재이용이나 배포의 경우, 이 저작물에 적용된 이용허락조건을 명확하게 나타내어야 합니다.
- 저작권자로부터 별도의 허가를 받으면 이러한 조건들은 적용되지 않습니다.

저작권법에 따른 이용자의 권리는 위의 내용에 의하여 영향을 받지 않습니다.

이것은 [이용허락규약\(Legal Code\)](#)을 이해하기 쉽게 요약한 것입니다.

[Disclaimer](#)

A THESIS  
FOR THE DEGREE OF MASTER OF SCIENCE

**The protective effects of Ginsenoside-Rg3 on lipopoly  
saccharide-induced suppression of brown and beige a  
dipose thermogenesis**

**Fang Feng**

Department of Food Science and Nutrition

GRADUATE SCHOOL  
JEJU NATIONAL UNIVERSITY

February 2023

# The protective effects of Ginsenoside-Rg3 on lipopoly saccharide-induced suppression of brown and beige a dipose thermogenesis

**Fang Feng**

(Supervised by Professor Inhae Kang)

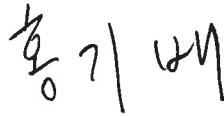
A dissertation submitted in partial fulfillment of the requirement for the degree  
of Master of Science

February 2023

This dissertation has been examined and approved by



Thesis director, Yunkyoung Lee, Prof. of Food Science and Nutrition, Jeju National University



Ki-Bae Hong, Prof. of Food Science and Nutrition, Jeju National University



Inhae Kang, Prof. of Food Science and Nutrition, Jeju National University

February 2023

Date

Department of Food Science and Nutrition  
GRADUATE SCHOOL  
JEJU NATIONAL UNIVERSITY

# Contents

<b>List of Abbreviations</b> .....	v
<b>List of Figure</b> .....	vii
<b>List of tables</b> .....	ix
<b>1. Introduction</b> .....	1
<b>2. Experimental section</b> .....	3
2.1 Experimental materials and sample preparation .....	3
2.2 Animal diets and treatment .....	3
2.3 Serum biochemistry .....	4
2.4 Hematoxylin and Eosin (H&E) staining .....	5
2.5 Cell culture and adipocyte differentiation.....	5
2.6 Isolation and culture of primary BAT and SubQ fat-derived mesenchymal stem cells.....	6
2.7 Oxygen consumption rate by Seahorse .....	6
2.9 Separation of proteins with western blotting.....	7
2.10 Analytical Statistics.....	8
<b>3. Results</b> .....	8

3.1 Rg3 protects from lipopolysaccharide (LPS)-induced adipocyte browning inhibition and BAT activation in primary brown and beige adipocytes.....	8
3.2 Rg3 improved fasting glucose and total cholesterol levels, but not most of the obesogenic parameters in LPS- CL316,243 (CL) challenged C57BL/6 mice .....	15
3.3 Rg3 promoted thermogenic activity in LPS and CL-treated C57BL/6 mice .....	25
<b>4. Discussion.....</b>	<b>31</b>
<b>5. Conclusion.....</b>	<b>34</b>
<b>6. References.....</b>	<b>35</b>

# Abstract

## The protective effects of Ginsenoside-Rg3 on lipopolysaccharide-induced suppression of brown and beige adipose thermogenesis

Fang Feng

Supervised by the Professor Inhae Kang

Department of Food Science and Nutrition Graduate School

JEJU NATIONAL UNIVERSITY

Ginsenoside Rg3 is the main component of Korean Red Ginseng (steamed *Panax ginseng* CA Meyer). Brown adipose tissue (BAT) is an important regulator of energy homeostasis to control obesity. Obesity is regarded as low-grade inflammation in adipose tissue, so finding the anti-inflammatory and immunomodulatory agents in white and BAT is a new challenge for obesity management. Rg3 is well known to have anti-inflammatory and anti-metabolic properties. However, it is unknown whether Rg3 protects against inflammation-induced browning inhibition or BAT activation. To answer this question, we used the primary culture of BAT as a BAT cell model and 3T3-L1 adipocytes or primary culture of Subcutaneous (SubQ) fat treated with cAMP analog were used for beige adipocyte cell models. Although Rg3 did not enhance brown adipogenesis, Rg3 reversed the attenuation of browning in lipopolysaccharide (LPS)-treated beige adipocytes and primary brown adipocytes by recovering uncoupling protein 1 (UCP1) and oxygen consumption rate compared to the LPS-treated group. We confirmed the protective effects of Rg3

against inflammation-induced inhibition of beige and BAT-derived thermogenesis in the animal model. CL316,243 (beta-adrenergic receptor agonist) and LPS were used to induce browning and inflammation, respectively. In C57BL/6 mice, Rg3 treatment (2.5 mg/kg BW for 8 weeks) effectively reversed LPS-induced inhibition of brown adipocyte features and alleviated hypercholesterolemia. As a result, these findings support the notion that Rg3-rich foods can act as browning agents to combat chronic inflammation and metabolic complications.

# List of Abbreviations

- ADRB3**, beta-3 adrenergic receptor
- AMPK**, AMP-activated protein kinase
- BAT**, Brown adipose tissue
- BW**, Body weight
- BWG**, BW gain
- C/ebp $\alpha$** , CCAAT/enhancer-binding protein alpha
- cAMP**, 8-Bromo-Camp
- CL**, CL316,243
- CLS**, crown-like structure
- DMEM**, Dulbecco's Modified Eagle's Medium
- DMSO**, Dimethyl sulfoxide
- FA**, fatty acid
- FBS**, fetal bovine serum
- FCCP**, carbonyl cyanide 4-trifluoromethoxy phenylhydrazone
- GTT**, glucose tolerance test
- IRS**, insulin receptor substrate
- LPS**, Lipopolysaccharide
- mtDNA**, mitochondrial DNA
- NLRP3**, NLR family pyrin domain containing 3
- Nrf2**, nuclear factor erythroid 2-related factor 2
- OXPHOS**, oxidative phosphorylation
- Pgc1 $\alpha$** , peroxisome proliferator-activated receptor- $\gamma$  coactivator1 $\alpha$
- PI3K**, phosphatidylinositol-3-kinase



**Ppar $\gamma$** , proliferator- activated receptor gamma

**RGE**, Red Ginseng Extract

**Rg3**, Ginsenoside Rg3

**Sirt1**, Sirtuin 1

**SubQ**, subcutaneous fat

**TC**, total cholesterol

**TFAM**, mitochondrial transcription factor A

**TRL4**, toll like receptor 4

**UCP1**, uncoupling protein 1

**VDAC**, voltage-dependent anion channel

**WAT**, white adipose tissue

# List of Figure

<b>Fig 1.</b> Rg3 enhanced mitochondrial activation in BAT mesenchymal stem cells (MSCs) by upregulation mitochondrial oxygen consumption.....	10
<b>Fig 2.</b> Rg3 enhanced mitochondrial activation with UCP1 expression by Western blot analysis	11
<b>Fig 3.</b> Rg3 treatment simultaneous induction with cAMP would increase the number of mitochondria-expressed cells .....	12
<b>Fig 4.</b> Effect of Rg3 recovers LPS-induced inhibition of browning gene expression of UCP1, PGC1a by qPCR.....	13
<b>Fig 5.</b> Effect of Rg3 recovers LPS-induced inhibition of browning gene expression of UCP1, by qPCR and thermogenesis-related proteins by Western blot.....	14
<b>Fig 6.</b> Rg3 reduces lipopolysaccharide (LPS)-mediated inflammatory responses in C57BL/6 mice. ....	16
<b>Fig 7.</b> Mice Body weight (BW) and BW gain (BWG) were not affected by either groups.....	17
<b>Fig 8.</b> Mice tissue mass were not affected by either groups. ....	18
<b>Fig 9.</b> Rg3 improves fasting glucose levels in LPS- CL316,243 (CL)-challenged C57BL/6 mice. ....	19
<b>Fig 10.</b> Rg3 improves TC levels in LPS- CL316,243 (CL)-challenged C57BL/6 mice. ....	20
<b>Fig 11.</b> Liver H&E staining and TG,TC no significant difference was observed among the groups. ....	21
<b>Fig 12.</b> Epididymal adipose H&E staining and adipose size no significant difference .....	22
<b>Fig 13.</b> Rg3 treatment dropped down the crown-like structure (CLS) numbers.....	23
<b>Fig 14.</b> Rg3 reduced inflammatory markers such as F4/80 and Mcp1mRNA expressions .....	24
<b>Fig 15.</b> Rg3 group showed more resist temperature upon LPS treatment .....	26

**Fig 16.** Rg3 treated group showed smaller lipid droplets size both BAT and SubQ WAT by H&E staining..... 27

**Fig 17.** Thermogenic gene expression and the mitochondrial DNA (mtDNA) contents was increased in SubQ fat by Rg3..... 28

**Fig 18.** Effect of Rg3 increased protein expressions by Western blot analysis. .... 29

**Fig 19.** Rg3 recovers LPS-induced inhibition of browning by upregulation mitochondrial oxygen consumption..... 30

# List of tables

**Table 1.** Dietary composition of high-fat (HF) ..... 41

**Table\_2.** Primer sequences for real-time PCR ..... 42

## 1. Introduction

Obesity is defined as an excessive fat accumulation that leads to chronic low-grade inflammation [1]. Adipocyte inflammation is mechanistically linked to metabolic disease and organ complications, increasing the risk of several diseases, such as diabetes, heart disease, and some cancers [2]. Although the pathways to obesity and/or adipocyte inflammation are well-reported and confirmed, there are still gaps of knowledge that remain to be elucidated. Adipose tissue is a complex endocrine organ to regulate the whole body's homeostasis. White adipose tissue (WAT) and brown adipose tissue (BAT) are the two forms of adipose tissue, that possess opposing functions. WAT has a fundamental role as an energy reservoir to control several metabolic pathways, such as food intake and immune cell function [3, 4]. BAT is a critical regulator of energy homeostasis to burn energy into heat via uncoupling protein 1 (UCP1) protein and it is responsible for ~ 20% of total energy expenditure through non-shivering thermogenesis [5, 6]. WAT from specific depots such as subcutaneous (SubQ) fat undergo being or browning (beige fat development) upon appropriate stimuli, which mimics the characteristics of BAT; the beige fat (white fat converting BAT) has multilocular lipid droplets and multiple mitochondria with UCP1 expression [7]. Recent evidence demonstrated that toll-like receptor 4 (TLR4) and NLR family pyrin domain containing 3 (NLRP3) inflammasome activation inhibited adaptive thermogenesis induced by cold exposure or beta-adrenergic receptor (ADRB3) agonists via endoplasmic reticulum (ER) stress [8, 9]. Given that obesity is thought to be a low-grade inflammatory state in adipose tissue, dietary supplements that guard against inflammation-induced suppression of BAT/beige fat growth may be effective pharmaceutical treatments for obesity.

Ginseng, the root of *Panax ginseng Meyer*, has been widely used herbal plant for bio-medicinal purposes in China and South Korea which were discovered over 2-5000 years ago [10, 11]. White ginseng refers to freshly harvested ginseng, and processed red ginseng refers to

steamed ginseng are two different ginseng that mostly consumed in Asian country. Steaming (steamed at 90–100°C for 2–3 h) of fresh ginseng without peeling the roots and drying [12], leads to a change in the types and contents of ginsenosides [13-15]. Ginsenosides, the unique components of ginseng, are saponins and a class of steroid glycosides contained in ginseng. The structure of ginsenosides differ depending on stereo-specificity and the number or position of sugar moieties such as glucose, xylose, arabinose, and rhamnose attached to carbon [16, 17]. Although the absorption rate of ginsenosides and their metabolites in intestine is shallow, ginsenosides are well reported to possess strong pharmacological activities such as anti-inflammation [18] and anti-cancer [19]. Among many ginsenosides, ginsenoside Rg3 exists in high content in red ginseng compared to white ginseng. It is well studied the role of Rg3 in anti-cancer, anti-diabetic and anti-oxidants with immune-modulation effects [19-21]. Anti-adipogenic effects of Rg3 have been reported such as inhibition of adipocyte differentiation; [22, 23] and enhanced glucose uptake via the phosphatidylinositol-3-kinase (PI3K) – insulin receptor substrate (IRS) pathways [24]. Not only *in vitro* data, but several researchers investigated the anti-obesity effects of dietary intake of Rg3 in an animal model. Rg3 intake (0.1 [23] 10 mg [25] Rg3/kg diet, 8 weeks) significantly reduced body weight and fat content with the improvement of hepatic steatosis by regulating PPAR- $\gamma$  and C/EBP- $\alpha$  expressions. Kim et al. Reported that Rg3 activates beige adipogenesis in 3T3-L1 adipocytes via AMP-activated protein kinase (AMPK) signaling pathways [26]. However, it is unknown whether Rg3 protects against inflammation-induced inhibition of browning or BAT activation.

Therefore, we posited that Rg3 would prevent inflammation-induced inhibition of browning and protect against HF diet. To answer this hypothesis, we established a rigorous beige adipocyte cell model by using 3T3-L1 cells and SubQ fat-derived mesenchymal stem cells (MSCs) differentiated into adipocytes with 8-Br-cAMP. For the brown adipocyte cell model, BAT-derived MSCs were utilized to investigate the role of Rg3 on inflammation-induced BAT activation. Both

beige and brown adipocytes cells models challenged LPS to induce inflammation. In vivo model, Rg3 (2.5 mg/kg BW, 8 weeks) was injected into high fat (HF) diet-fed C57BL/6 mice with or without LPS followed by  $\beta$ 3 agonist CL-316,243 treatment to induce browning. Here, we thoroughly assessed the metabolic changes by Rg3 in the BAT and beige adipocytes upon chronic inflammation.

## **2. Experimental section**

### ***2.1 Experimental materials and sample preparation***

Except when otherwise noted, all cell culture dishes were purchased from SPL (Seoul, Korea). Dulbecco's Altered Falcon's Medium (DMEM), fetal ox-like serum (FBS), and penicillin/streptomycin were bought from Gibco (Fabulous Island, NY, USA). Rosiglitazone (BRL 49653) was bought from Cayman Substance (Ann Arbor, MI, USA). Any remaining synthetic substances and reagents were bought from Sigma Compound Co. (St. Louis, MO, USA) except if generally expressed. We bought ginsenoside Rg3 (Rg3) from Sigma Chemical Co. (St. Louis, MO, USA). Before using a 40 mM Rg3 stock in animal research and primary cell culture, we freshly diluted it with DMSO.

### ***2.2 Animal diets and treatment***

All conventions and strategies were supported by the Institutional Creature Care and Use Committee of the Jeju National University (Endorsement ID # 2021-0026). 6-10-week-old C57BL/6J mice were bought from the ORIENT BIO Creature Center (Seongnam-si, Korea) and housed in a dull/light cycle at Jeju Public College and permitted to polish-off water and a standard chow diet not obligatory. For the Rg3 animal experiment, C57BL/6 mice were allowed to consume the high-fat diet (HF, 60% kcal from fat) *ad libitum* for 12 weeks. Mice were divided into 4

different groups: high fat (HF, n=6), HF + CL316,243 (CL, 1 mg/kg, n=4), HF + CL+LPS (CL+LPS, 7.5 µg/mouse, n=5), or HF +CL+LPS+Rg3 (LPS+Rg3, 2.5 mg/kg, n=6). Mice were intraperitoneally (i.p.) injected with saline or the  $\alpha$ -3 adrenergic receptor agonist CL 316,243 (Santa Cruz Biotechnology, 1 mg/kg BW) every day for 8 days to cause adipose tissue browning; To induce inflammation, 7.5 µg/mouse i.p. injection for 5 days; For Rg3 treatment, i.p. injection of 2.5 mg/kg BW Ginsenoside Rg3 (dissolved in DMSO) treated HF-fed mice for 8 weeks starting from week 4. To gauge the thermogenic potential the internal heat level was estimated utilizing an infrared (IR) thermometer (Promotion 801, Zhengzhou AiQURA Shrewd Innovation Co., Henan, China) beforehand [28]. An IR camera (FLIR E5, FLIR® Frameworks, Wilsonville, OR, USA) was utilized to distinguish and catch the warm delivery in the body surface as recently portrayed [8]. The surface intensity discharge temperature between 29-34 °C was shown utilizing FLIR Exploration IR programming.

### **2.3 Serum biochemistry**

Following the completion of the experiment, the experimental animals were fasted for 12 hours before being sacrificed via carbon dioxide narcosis. A heart puncture was used to collect blood, and serum samples were divided up. Using an enzyme assay kit (Asan Pharmaceutical Co., Seoul, Korea) with absorbance at 550 nm, the levels of total serum cholesterol (TC, mg/dL) and triglycerides (TG, mg/dL) were measured. Before sacrifice, subjects were given a 12-hour fast, and blood glucose levels were assessed using a glucose meter (Medium Blood Glucose Analyzer, Kia Ace Co., Ltd., Gyeonggi, Korea).



#### ***2.4 Hematoxylin and Eosin (H&E) staining***

Upon necropsy, brown fat, subcutaneous (SubQ) fat, epididymal fat, and liver tissue were gathered from the mice and flash-fixed in 10% cushioned formalin. Paraffin-installed tissues were cut into 5-7 $\mu$ m areas and handled for hematoxylin and eosin (H&E) staining, as depicted already [29]. Splendid field pictures were acquired by an Invitrogen magnifying instrument (Invitrogen™ EVOS™ FL Advanced Rearranged Fluorescence Magnifying instrument, Invitrogen, CA, USA) under 10X, 20X amplification.

#### ***2.5 Cell culture and adipocyte differentiation***

The experiment's 3T3-L1 preadipocytes came from the American Type Culture Collection (Manassas, VA, USA). Cells were grown in DMEM (Gibco BRL, Dulbecco's Modified Eagle's Medium) with 10% fetal calf serum (FCS) and 1% penicillin/streptomycin (P/S) supplements at 37°C and 5% CO<sub>2</sub>. After confluence was reached, 10% Fetal Bovine Serum (FBS, Invitrogen, Carlsbad, CA, USA) was substituted for the growth medium to facilitate differentiation. After 48 hours (day 0), 500  $\mu$ M IBMX, 1  $\mu$ M Dex, 2nM insulin (MDI), and 10% FBS were added to DMEM to induce differentiation for 48 hours after treatment with the extract. After 48 hours (day 2), 2 nM insulin and 10% FBS were added to the extract in DMEM, the extract was incubated for 48 hours, and the medium was changed every 24-48 hours until the desired degree of differentiation. To determine the effects of Rg3 on late phase of adipogenesis, Rg3 was treated in mature adipocytes. 3T3-L1 adipocytes were cultured until they became mature adipocytes, then Rg3 was treated for 3-7 days. The medium was changed every 24-48 hours.

## ***2.6 Isolation and culture of primary BAT and SubQ fat-derived mesenchymal stem cells***

BAT and SubQ-MSCs were secluded from interscapular earthy-colored fat or subcutaneous fat of C57BL/6 mice individually. Fat tissues were taken apart and put into a collagenase processing support. After 15 min at 37° C in a shaking water shower, tissue remainders were eliminated by filtration through a 100 µm nylon network and put on ice for 30 min. The BAT or SubQ-MSCs were separated through a 30 µm nylon network and centrifuged at 400 g for 10 min. Resuspended in a separation medium at the pellet. Cells were cultivated on 96/12-well plates (day 0) and developed at 37° C under 5% CO<sub>2</sub> condition. For separation, the medium was traded each 24 h until day 7. Briefly, Preadipocytes should be switched to induction media once they have reached 100% confluence (day 0). For BAT MSCs differentiation medium, DMEM 10% FBS supplemented with 200 nM insulin, 5 µM Dex, 0.5 µM of 3-isobutyl-1-methylxanthine, 1 µM Triiodothyronine (T3) and 0.125 µM of indomethacin were added to cultures. After 48 hours, 20 nM insulin and 1 µM T3 were added to cells for additional 2 days. For the SubQ MSC differentiation medium, DMEM 10% FBS supplemented with 1.7 nM insulin, 1 µM Dex, and 500 µM of 3-isobutyl-1-methylxanthine were added to cultures. Then, a fresh medium containing 1.7 nM insulin and 1 µM of rosiglitazone brl 49653 was added to cells for additional 2 days. After 48 h, the media was replaced for 3-5 days by DMEM containing 10% FBS.

## ***2.7 Oxygen consumption rate by Seahorse***

The oxygen consumption rate (OCR) in 3T3-L1 adipocytes, BAT, and SubQ fat-derived primary cells was measured using an XF24 extracellular flux analyzer (Agilent Technologies) at Jeju National University's Bio-Health Materials Core-Facility, as previously described. [30]. Momentarily, cells were cultivated in an XFe analyzer microplate (24-well) and refined until they arrived at confluency. The isolated adipocytes that had been treated without Rg3 were exchanged for XF base media before tests that were amplified with 10 mM glucose, 2 mM glutamine, and 1

mM pyruvate were conducted. To estimate the turnover of adenosine triphosphate (ATP), cells were given oligomycin (oligo, 2 M) treatment. Using FCCP (0.5 M), a 4-trifluoromethoxy phenylhydrazone derivative of carbonyl cyanide, the most extreme respiratory limit was determined. Then, a mixture of antimycin A (1 M) and rotenone (1 M) (A+ R) inhibited mitochondrial oxygen use.

### ***2.8 Real-time Polymerase Chain Reaction analysis of mRNA (real time-PCR)***

After the finish of the examination, 0.2 g of the fat tissue was put away quickly in the cooler, and cells were exposed to RNA extraction utilizing Trizol reagent (Invitrogen Co., Carlsbad, CA, USA). cDNA was blended by high-limit cDNA switch record units (Applied Biosystem, USA) in wake of estimating the separated RNA fixation utilizing a nanodrop (Nano-200 Miniature Spectrophotometer, Hangzhou City, China). Quality still up in the air by ongoing PCR (CFX96™ Continuous PCR Identification Framework, Bio-Rad, USA). The overall quality articulation was standardized hypoxanthine-guanine phosphoribosyltransferase (HPRT) and additionally ribosomal protein sidelong tail subunit P0 (RPLP0, 36B4) (Cosmo Genetech, Table 2).

### ***2.9 Separation of proteins with western blotting***

Tissue samples were homogenized with a homogenizer in ice-cold radioimmunoprecipitation assay lysis buffer (RIPA) (Thermo Fisher Scientific) containing a protease and phosphatase inhibitor cocktail (Sigma-Aldrich) before centrifugation to collect the supernatant. Proteins (10-12 g) were separated by 10% SDS-PAGE and transferred to PVDF membranes (Thermo Fisher Scientific) with Tris-buffered saline/Tween 20. (TBST). The membranes were blocked at room temperature for 1 hour. The membranes were washed several times with TBST solution before being incubated overnight at 4°C with primary antibodies against

PPAR, UCP1,  $\beta$ -actin (Cell Signaling Technology, Danvers, MA, USA), adipocyte protein 2 (aP2, FABP4) (Santa Cruz Biotechnology), mitochondrial transcription factor A (TFAM) (Abcam, Cambridge, UK), or voltage-dependent anion channels (VDAC, Cell Signaling Technology). The membranes were washed several times the next day before being incubated for 1 hour with the secondary antibodies goat anti-rabbit (Cell Signaling Technology) or goat anti-mouse IgG-HRP (Santa Cruz Biotechnology). Following that, the membranes were washed and incubated with an enhanced chemiluminescence reagent (ECL, Perkin Elmer). ChemiDoc MP (Bio-Rad) was used to visualize the bands, and Image Lab (Bio-Rad) or Image J was used to calculate the expression level (NIH, MD, USA)

## ***2.10 Analytical Statistics***

The trial's outcomes are communicated as the mean  $\pm$  standard blunder of the mean (SEM). Statistical calculations were performed utilizing ANOVA (one-way examination of difference) with Bonferroni's different correlation test or understudy's t-test. P-esteem  $<0.05$  was thought of as genuinely huge. All examinations were performed with GraphPad Crystal 8.0.2 (La Jolla, California., USA).

## **3. Results**

### ***3.1 Rg3 protects from lipopolysaccharide (LPS)-induced adipocyte browning inhibition and BAT activation in primary brown and beige adipocytes***

Previously, our group reported that Rg3 inhibited adipogenesis in 3T3-L1 adipocytes, And Rg3 suppressed both early-phase and terminal adipogenesis with fatty acid oxidation. These results suggested that by encouraging FA oxidation and mitochondrial activity, Rg3 prevents fat formation in adipocytes. Next we wondered whether Rg3 would promote brown adipogenesis and

white adipocyte browning. To verify this claim, murine primary brown adipocytes (BAT MSCs) from BAT was treated with or without Rg3 (60  $\mu$ M) during brown adipogenesis. Rg3 treatment showed significant enhancement of mitochondrial bioenergetics, as evidenced by an increase in basal, maximal, and uncoupling oxygen consumption rate (OCR) with ATP production (Fig. 1). The increase in OCR was followed by the induction of UCP1 protein level in Rg3-treated brown adipocytes (Fig. 2). Then, we established beige adipocytes by using primary subQ fat-derived adipocytes and 3T3-L1 adipocytes treated with 8-Bromo-cAMP (cAMP) [30, 34]. Rg3 treatment simultaneous induction with cAMP would increase the number of mitochondria-expressed cells compared to cAMP-treated beige adipocytes (Fig. 3). However, Rg3 treatment did not alter *Ucp1* and *Pgc1 $\alpha$*  mRNA level compared to cAMP-treated 3T3-L1 adipocytes (Fig. 4), which indicated that Rg3 did not induce beige adipogenesis. With our disappointment, we next postulated that Rg3 protects against inflammation-induced browning inhibition. To answer this hypothesis, lipopolysaccharide (LPS) was treated in a beige adipocyte model (3T3-L1 adipocytes with cAMP). Our data showed that the expressions of *Ucp1* and *Pgc1 $\alpha$*  levels were both reduced in LPS treated group while the expression of Rg3 treatment was a significant increase in beige adipocyte (Fig. 4). Consistently, *Ucp1* gene expression and mitochondrial transcription factor A (TFAM), voltage-dependent anion channel (VDAC), and oxidative phosphorylation (OXPHOS) complex II-V protein expression, but not complex I, were increased by Rg3 against LPS treatment in cAMP – treated primary beige adipocytes (Fig. 5).

## BAT MSCs

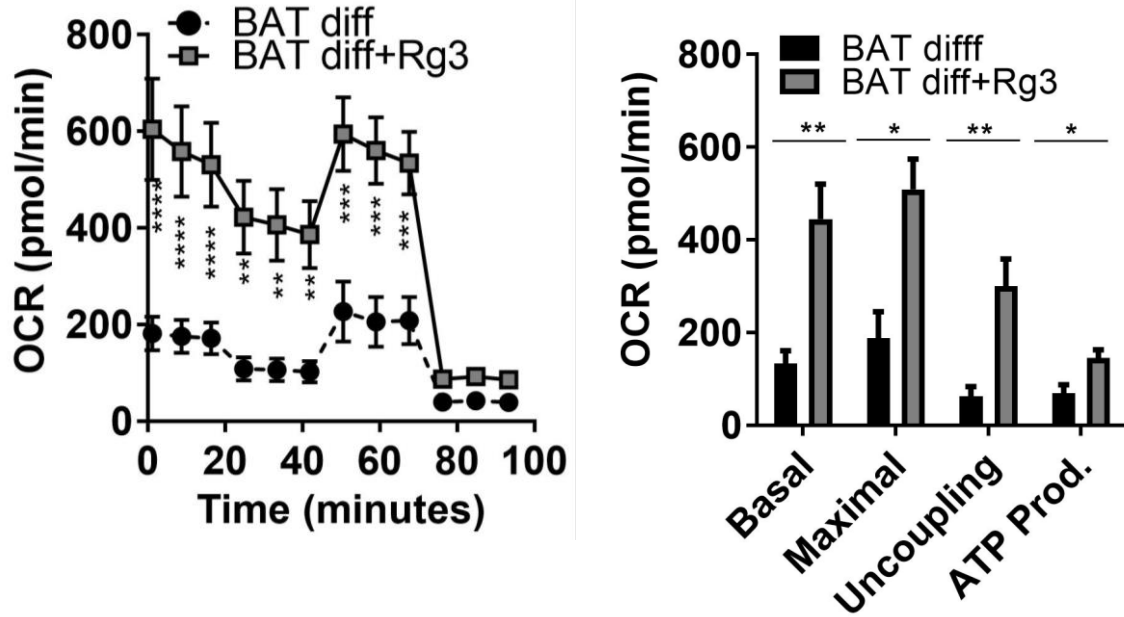


**Fig 1. Rg3 enhanced mitochondrial activation in BAT mesenchymal stem cells (MSCs) by upregulation mitochondrial oxygen consumption**

The oxygen consumption rate (OCR) in BAT mesenchymal stem cells (MSCs) treated with Rg3 as determined by Seahorse extracellular analyzer, the differentiation BAT MSCs were treated with or without Rg3 for 4 days;  $*p < 0.05$ ;  $**p < 0.01$ ; contrasted and the vehicle control by Understudy's *t*-test or one-way ANOVA with Bonferroni's examination test.

## BAT MSCs

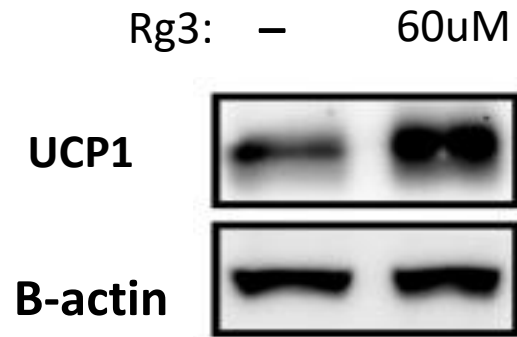


**Fig 2. Rg3 enhanced mitochondrial activation with UCP1 expression by Western blot analysis**

The level of UCP1 protein expression by western blot; the differentiation BAT MSCs were treated with or without Rg3 for 4 days; \* $p < 0.05$ ; \*\* $p < 0.01$ ; contrasted and the vehicle control by Understudy's *t*-test or one-way ANOVA with Bonferroni's examination test.

## SubQ MSCs

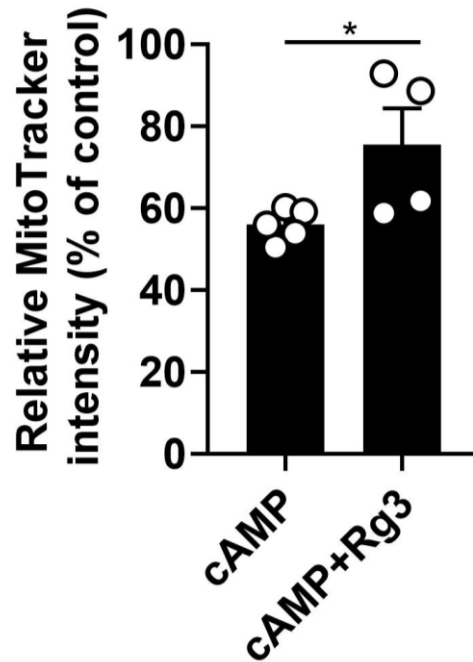


**Fig 3. Rg3 treatment simultaneous induction with cAMP would increase the number of mitochondria-expressed cells**

The abundance of mitochondria by MitoTracker fluorescence normalized to nuclear stain (NucBlue) (relative MitoTracker intensity, % of control);.  $*p < 0.05$ ;  $**p < 0.01$ ; contrasted and the vehicle control by Understudy's *t*-test or one-way ANOVA with Bonferroni's examination test.



### 3T3-L1

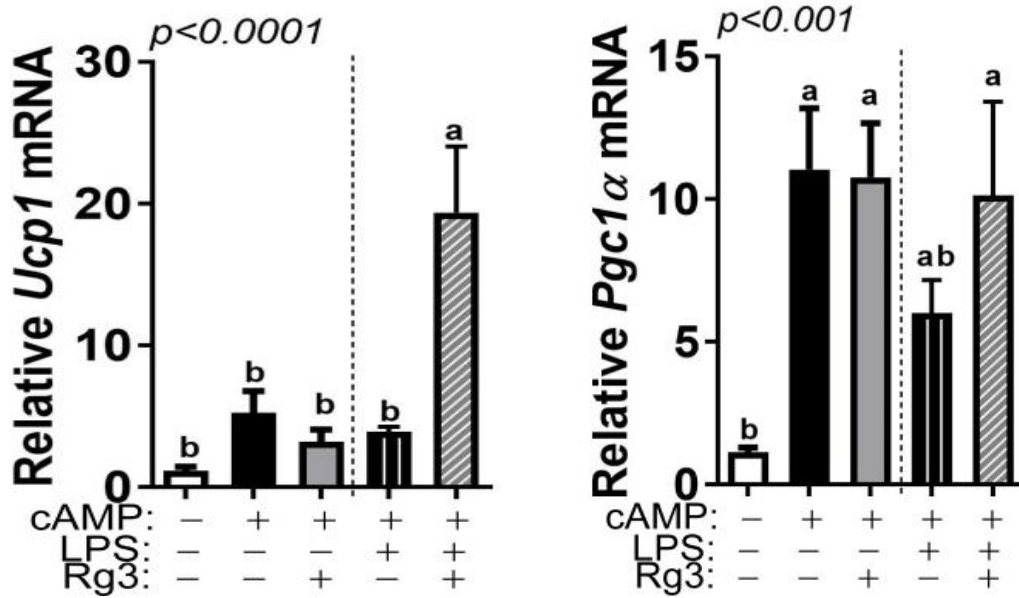


**Fig 4. Effect of Rg3 recovers LPS-induced inhibition of browning gene expression of UCP1, PGC1a by qPCR.**

Relative mRNA expression of Ucp1 and Pgc1α by real-time PCR; 3T3-L1 adipocytes were induced to differentiation in the presence or absence of Rg3 for 48 hours and treated LPS (100 ng/ml) for 72 hours followed by cAMP (0.5mM) stimulation for 4 hours; \* $p < 0.05$ ; \*\* $p < 0.01$ ; compared with the vehicle control by Student's *t*-test or one-way ANOVA with Bonferroni's comparison test.

## SubQ MSCs

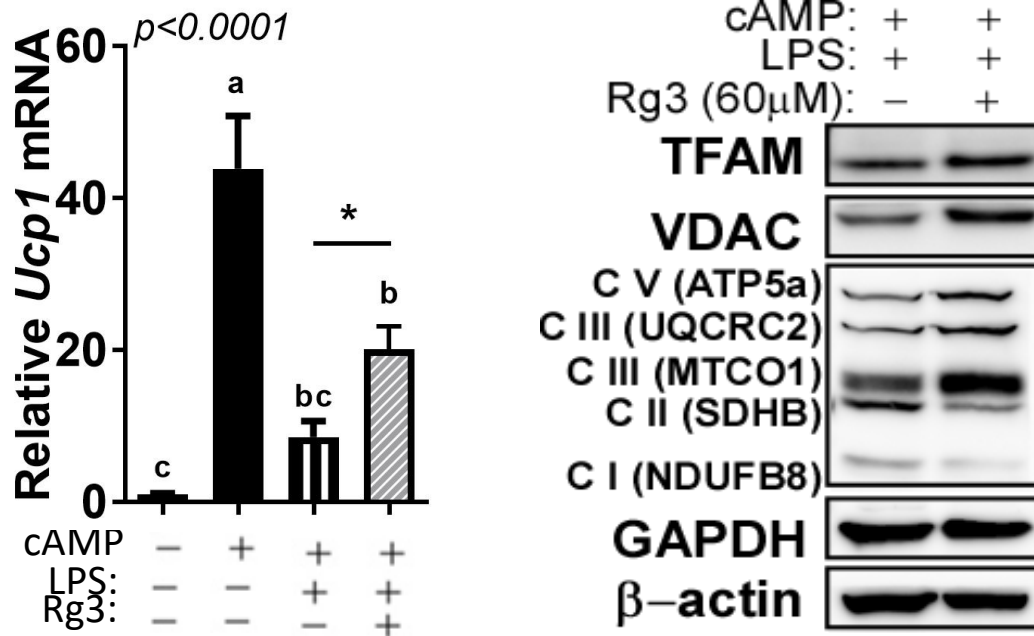
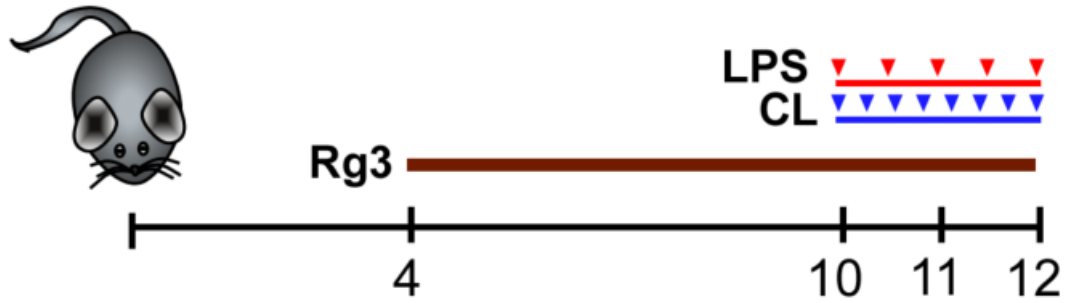


**Fig 5. Effect of Rg3 recovers LPS-induced inhibition of browning gene expression of UCP1, by qPCR and thermogenesis-related proteins by Western blot.**

Relative mRNA expression of Ucp1 by real-time PCR; And Immunoblots of thermogenesis-related proteins in the beige primary adipocytes from SubQ fat. Primary SubQ MSCs were induced to differentiation in the presence or absence of Rg3 for 48 hours and treated LPS (100 ng/ml) for 72 hours followed by cAMP (0.5mM) stimulation for 4 hours; \* $p < 0.05$ ; \*\* $p < 0.01$ ; *contrasted and the vehicle control by Understudy's t-test or one-way ANOVA with Bonferroni's examination test.*

### ***3.2 Rg3 improved fasting glucose and total cholesterol levels, but not most of the obesogenic parameters in LPS- CL316,243 (CL) challenged C57BL/6 mice***

To investigate the effects of Rg3 on brown and beige thermogenesis against inflammation, we performed a small animal study. CL316,243 (CL), beta-3 adrenergic receptor (ADRB3) agonist, and LPS were utilized to induce browning and inflammation, respectively. Mice were fed with an HF diet throughout the period for 12 weeks. Rg3 (2.5 mg/kg BW) was injected intraperitoneally into C57BL/6 mice for 8 weeks. LPS (7.5 µg/kg BW, every other days for 2 weeks) and CL (1 mg/kg BW, every consecutive 7 days) were injected as shown in (Fig.6). Body weight (BW) and BW gain (BWG) were not affected by either CL, CL+LPS or LPS+Rg3 in mice (Fig. 7). Liver, BAT and epididymal fat (E-WAT) mass also did not reach statistical significance in all the groups (Fig. 8). Despite no significant differences in BW, BWG and organ weight, the mice exhibited elevated levels fasting glucose levels in CL+LPS group, which was significantly improved by Rg3 treatment (Fig. 9). LPS-mediated elevated levels of serum total cholesterol (TC) which was also significantly improved by Rg3, but not serum triglyceride level (Fig. 10). Hepatic H&E staining showed lipid accumulation in the liver, but no difference among groups (Fig. 11) which was confirmed by hepatic TG and TC analysis (Fig. 11). Although there no differences in adipocyte hypertrophy (Fig. 12), the adipocyte inflammation which assess by crown-like structure (CLS) numbers were significantly dropped down by Rg3 treatment compared to CL+LPS groups (Fig. 13). Consistently, the inflammatory markers such as *F4/80* and *Monocyte chemoattractant protein-1(Mcp1)* mRNA expressions were significantly reduced by Rg3. *Interleukin 1β (Il-1β)* showed a similar trend, but there were no significant differences among the group (Fig. 14).



**HF:** High fat (60 % kcal from fat)  
**CL:** CL316,243 (1mg/kg)  
**CL+LPS:** HF+CL+LPS (7.5µg/kg)  
**LPS+Rg3:** HF+CL+LPS+Rg3 (2.5 mg/kg)

**Fig 6. Rg3 reduces lipopolysaccharide (LPS)-mediated inflammatory responses in C57BL/6 mice.**

Experimental scheme to evaluate the thermogenic effects of Rg3 against LPS in C57BL/6 mice. Rg3 (2.5 mg/kg BW) was injected intraperitoneally into C57BL/6 mice for 8 weeks. LPS (7.5 µg/kg BW) was administered to C57BL/6 mice every other day for 2 weeks. CL (1 mg/kg BW) was injected every day for 7 consecutive days; Data are expressed as mean ± SEM (n = 2-6) and analyzed using one-way ANOVA with Bonferroni's comparison test. Bars with different letters represent statistically significant differences. n.s. represents no significance, \* $p < 0.05$ .

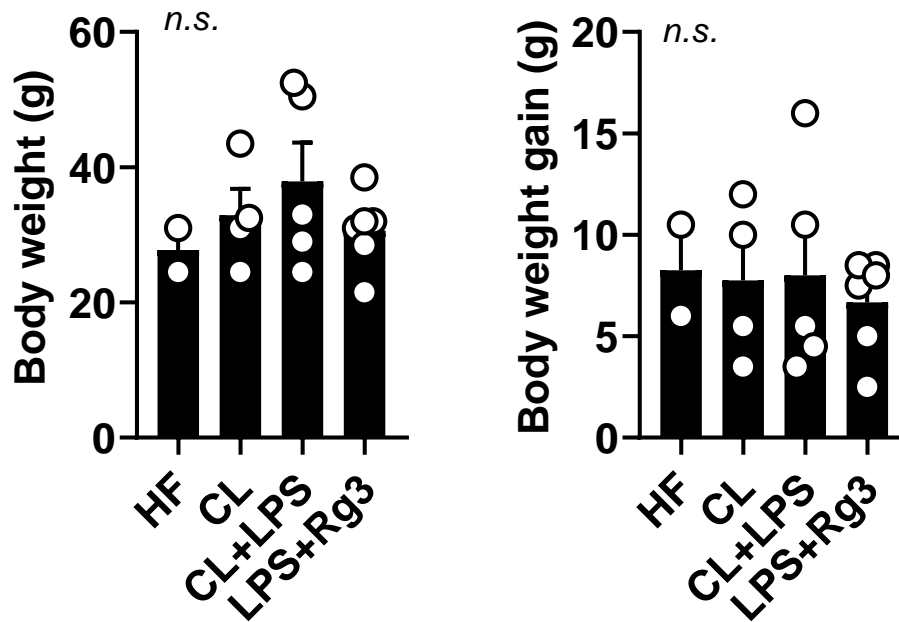


**Fig 7. Mice Body weight (BW) and BW gain (BWG) were not affected by either groups.**

C57BL/6 mice were fed an HF diet for 12 weeks; Data are expressed as mean  $\pm$  SEM (n = 2-6) and analyzed using one-way ANOVA with Bonferroni's comparison test. Bars with different letters represent statistically significant differences. *n.s.* represents no significance,  $*p < 0.05$ .

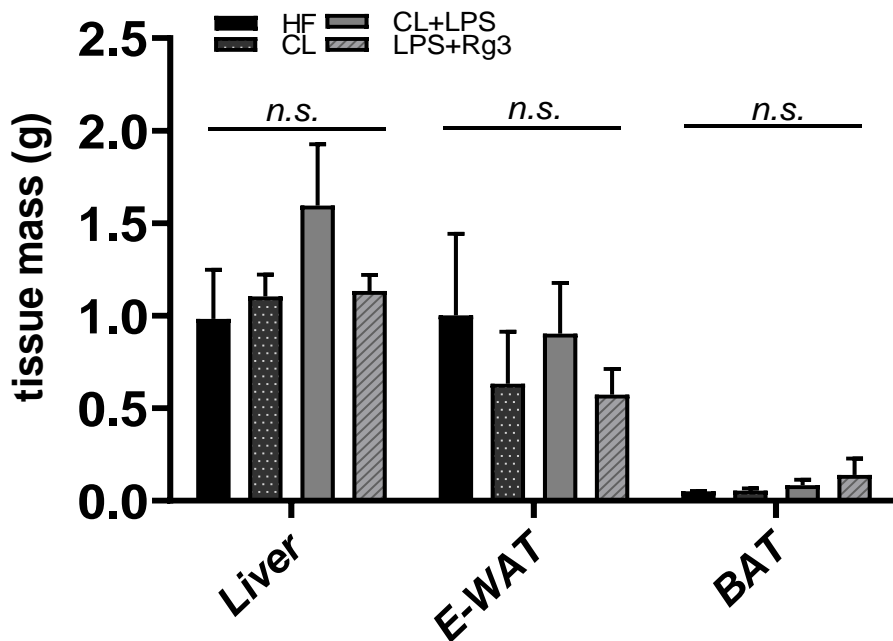


**Fig 8. Mice tissue mass were not affected by either groups.**

Liver, BAT, and epididymal fat (E-WAT) mass also did not reach statistical significance in all the groups; Data are expressed as mean  $\pm$  SEM (n = 2-6) and analyzed using one-way ANOVA with Bonferroni's comparison test. Bars with different letters represent statistically significant differences. *n.s.* represents no significance,  $*p < 0.05$ .

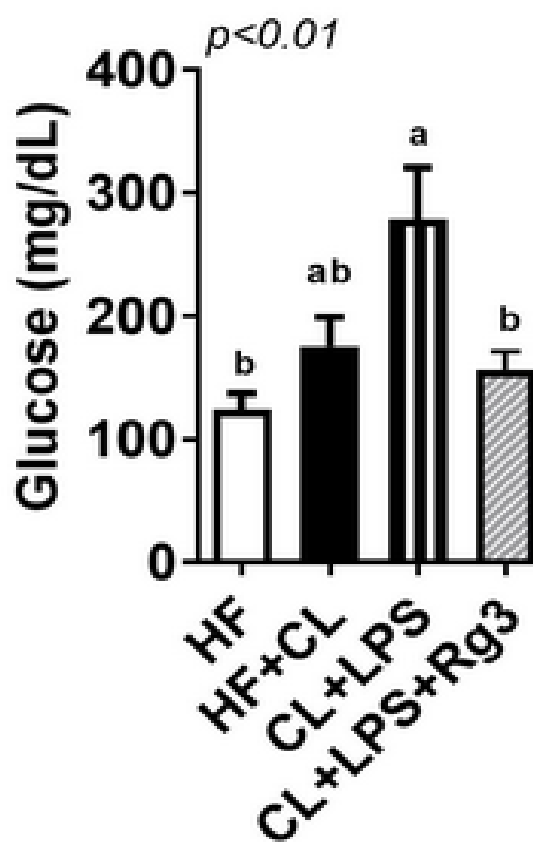


**Fig 9. Rg3 improves fasting glucose levels in LPS- CL316,243 (CL)-challenged C57BL/6 mice.** Fasting glucose (mg/dL); Data are expressed as mean  $\pm$  SEM (n = 2-6) and analyzed using one-way ANOVA with Bonferroni's comparison test. Bars with different letters represent statistically significant differences. *n.s.* represents no significance,  $*p < 0.05$ .

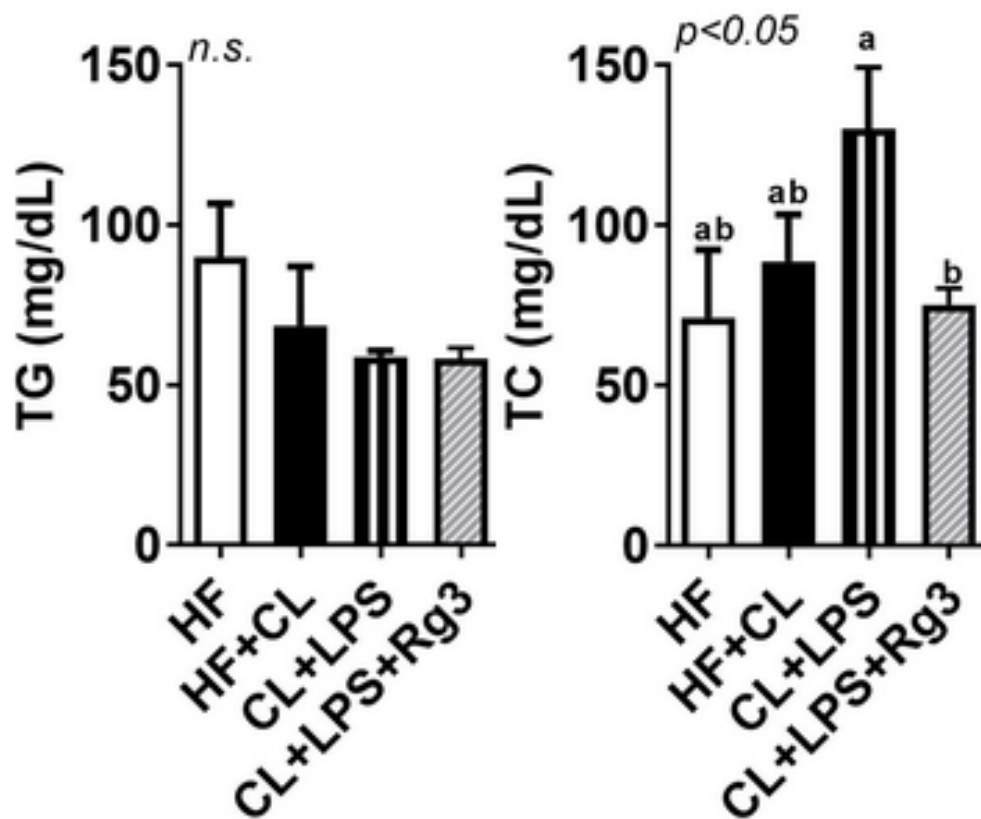


**Fig 10. 10 Rg3 improves TC levels in LPS- CL316,243 (CL)-challenged C57BL/6 mice.**

Triglycerides (TG) levels (mg/dL); Total cholesterol (TC) levels (mg/dL); Data are expressed as mean  $\pm$  SEM (n = 2-6) and analyzed using one-way ANOVA with Bonferroni's comparison test. Bars with different letters represent statistically significant differences. *n.s.* represents no significance,  $*p < 0.05$ .



## Liver

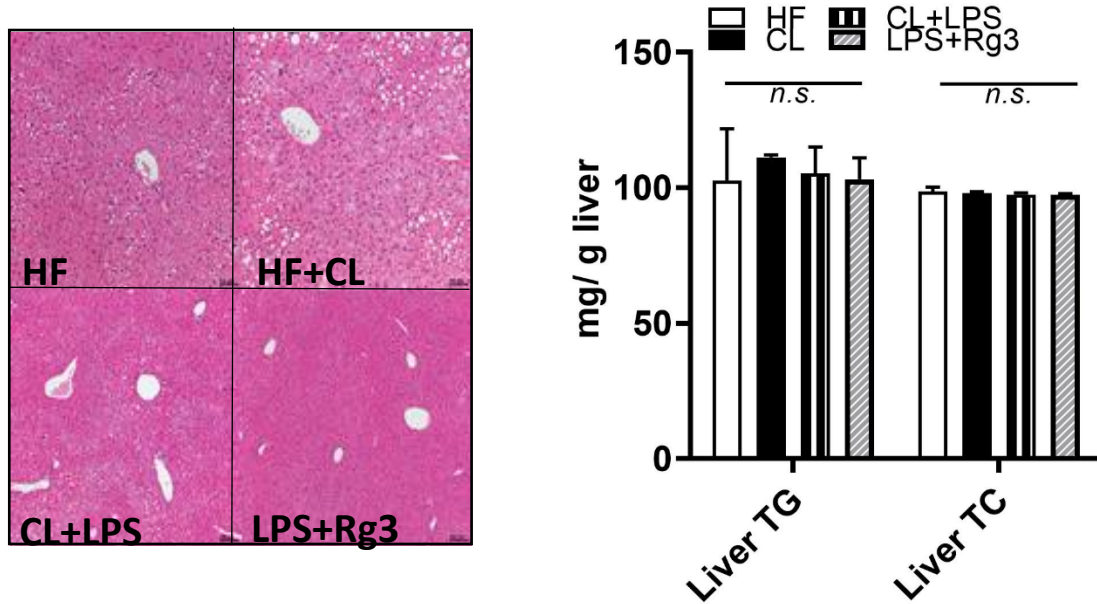


**Fig 11. Liver H&E staining and TG, TC no significant difference was observed among the groups.**

TG and TC levels (mg/g liver); Data are expressed as mean  $\pm$  SEM (n = 2-6) and analyzed using one-way ANOVA with Bonferroni's comparison test. Bars with different letters represent statistically significant differences. *n.s.* represents no significance,  $*p < 0.05$ .

## E-WAT

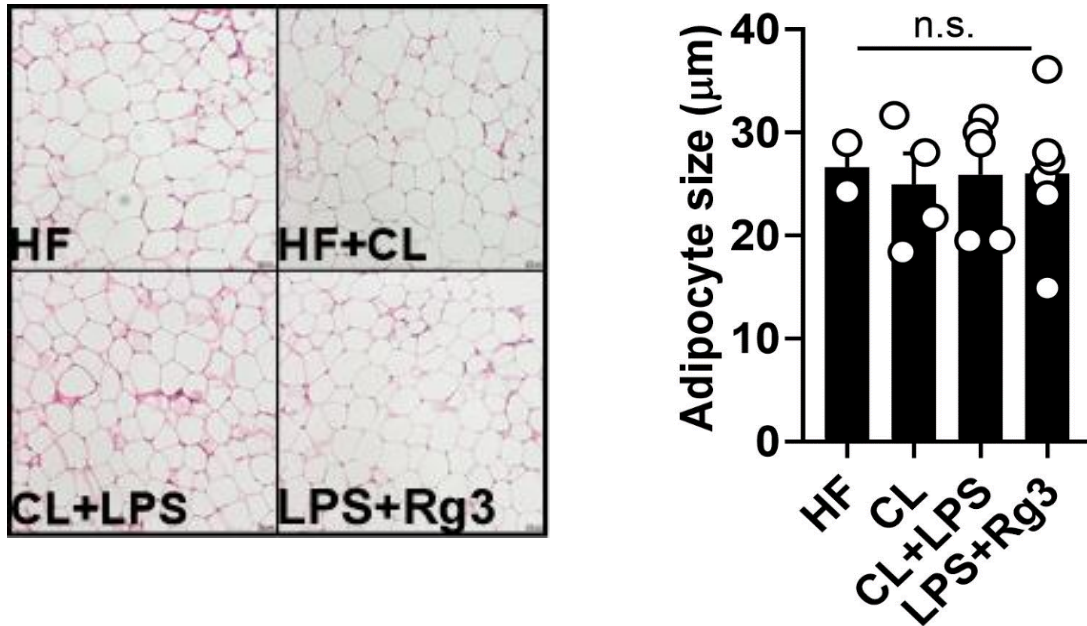


**Fig 12. Epididymal adipose H&E staining and adipocyte size no significant difference**

Representative H&E staining of epididymal adipose tissue (magnification, 10x); Data are expressed as mean  $\pm$  SEM (n = 2-6) and analyzed using one-way ANOVA with Bonferroni's comparison test. Bars with different letters represent statistically significant differences. *n.s.* represents no significance,  $*p < 0.05$ .

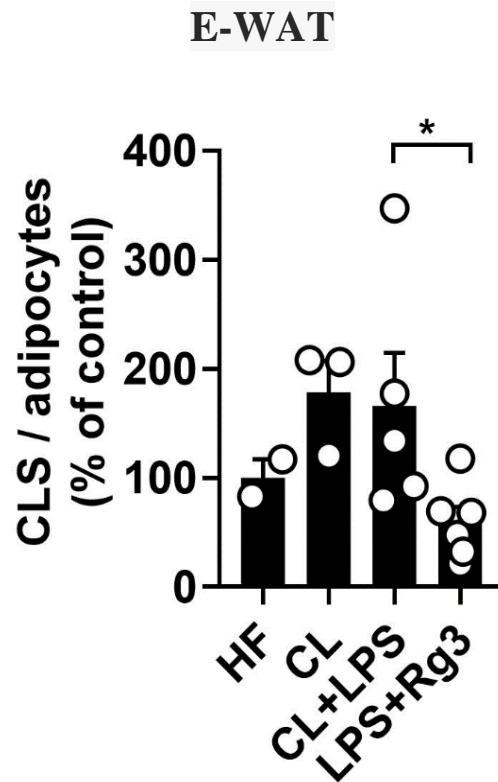


**Fig 13. Rg3 treatment dropped down the crown-like structure (CLS) numbers**

The number of crown-like structures (CLS) of epididymal adipose tissue sections in total adipocytes (% of control); Data are expressed as mean  $\pm$  SEM (n = 2-6) and analyzed using one-way ANOVA with Bonferroni's comparison test. Bars with different letters represent statistically significant differences. *n.s.* represents no significance,  $*p < 0.05$ .

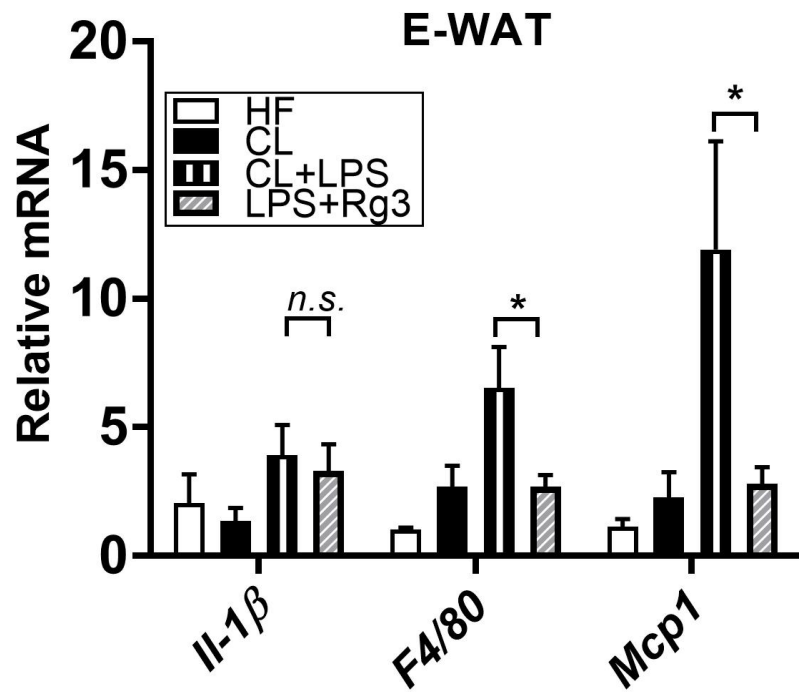


**Fig 14. Rg3 reduced inflammatory markers such as F4/80 and Mcp1mRNA expressions**

Relative mRNA expression of *Il-1  $\beta$* , *F4/80*, and *Mcp1* by real-time PCR.; Data are expressed as mean  $\pm$  SEM (n = 2-6) and analyzed using one-way ANOVA with Bonferroni's comparison test. Bars with different letters represent statistically significant differences. *n.s.* represents no significance, \**p* < 0.05.

### ***3.3 Rg3 promoted thermogenic activity in LPS and CL-treated C57BL/6 mice***

To further validate the promoting effects of Rg3 on thermogenesis in mice, adaptive thermogenic features were measured in brown or beige fat of C57BL/6 mice. Rg3 treated group showed more resist temperature upon LPS treatment compared with the CL+LPS group, indicating that Rg3 may have a potential thermoregulatory function (Fig. 15). Thermographic imaging of these mice confirmed the increased surface temperature of SubQ and interscapular BAT (Fig. 15). The size of lipid droplets in both BAT and SubQ WAT, which observed by H&E staining, showed smaller lipid droplets size in Rg3 treated group (Fig. 16). Although brown-specific *Ucp1* gene expression was insufficient to reach statistical significance in the Rg3-treated group, thermogenic gene expression in SubQ fat, including *Pgcl $\alpha$*  and *Cidea*, was increased in Rg3 treatment following CL and LPS exposure. (Fig. 17). Consistent trend was found in protein expression of UCP1 and PGC1 $\alpha$  in SubQ fat by Rg3 (Fig. 17). With our expectation, the mitochondrial DNA (mtDNA) contents are low in SubQ fat of CL+LPS-treated mice compared to CL group, which was recovered by Rg3 treatment (Fig. 17) with increased OXPHOS mitochondrial complex (Fig. 18). Although the Rg3's BAT activation against LPS which evidenced by UCP1 and PGC1 $\alpha$  protein level was subtle, we assumed that mitochondrial activation may be involved in the protection of LPS-mediated inhibition of browning. Strikingly, Rg3 treatment for 4 days in fully differentiated BAT-derived primary adipocytes promoted the overall mitochondrial respiration rate (Fig. 18). These data suggest that Rg3 reversed inflammation and adipocyte browning in the presence of LPS with mitochondrial activation.

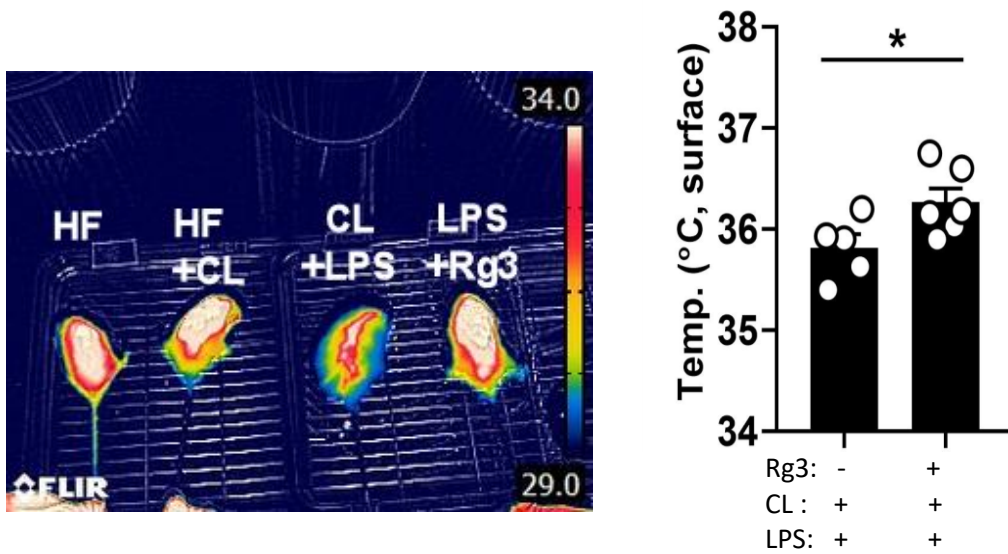


**Fig 15. Rg3 group showed more resist temperature upon LPS treatment**

Thermographic photo to measure heat production after 8 weeks of Rg3 treatment; The temperature of the mice's surface region after 8 weeks of Rg3 treatment; Data are expressed as mean  $\pm$  SEM (n = 2-6) and analyzed using one-way ANOVA with Bonferroni's comparison test. Bars with different letters represent statistically significant differences. *n.s.* represents no significance, *\*p* < 0.05.

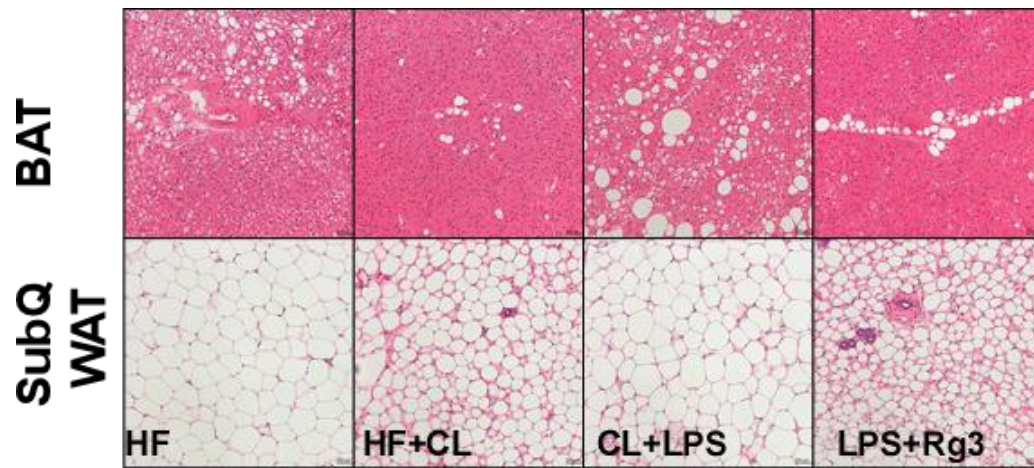


**Fig 16. Rg3 treated group showed smaller lipid droplets size both BAT and SubQ WAT by H&E staining**

BAT and SubQ WAT sections stained using H&E (magnified 20x) with scale bars=100  $\mu$ m; Data are expressed as mean  $\pm$  SEM (n = 2-6) and analyzed using one-way ANOVA with Bonferroni's comparison test. Bars with different letters represent statistically significant differences. *n.s.* represents no significance, *\*p* < 0.05.

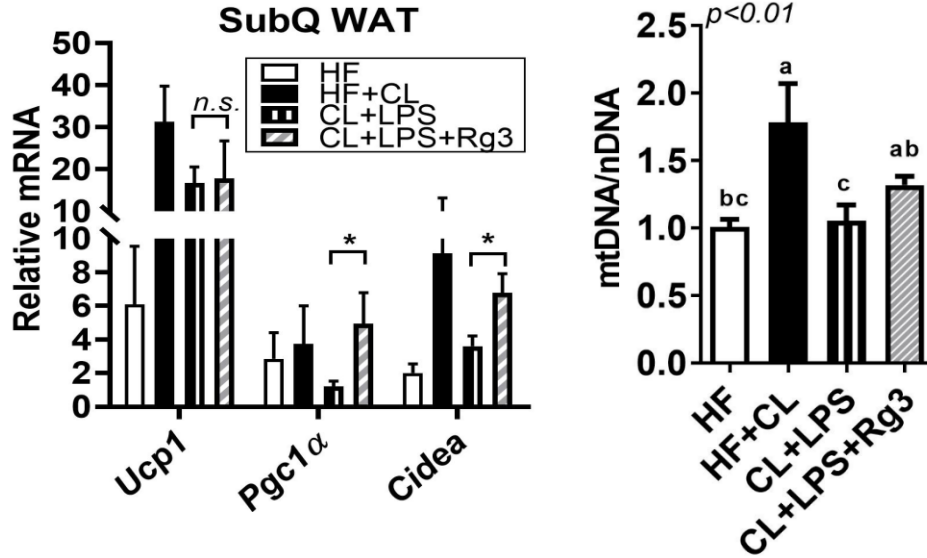
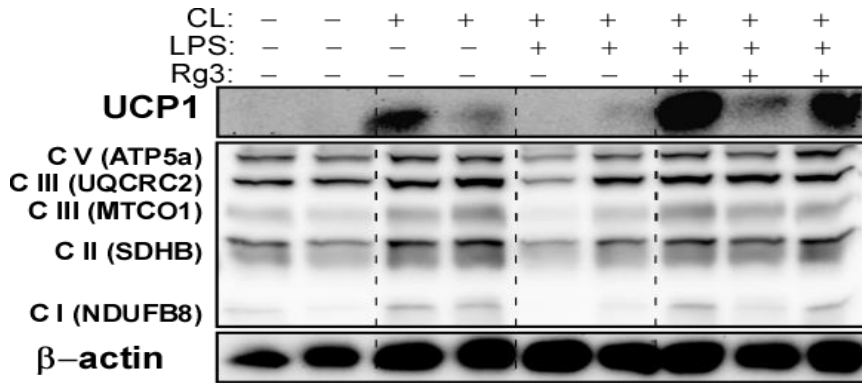


**Fig 17. Thermogenic gene expression and the mitochondrial DNA (mtDNA) contents was increased in SubQ fat by Rg3**

Levels of mtDNA/nDNA by real-time PCR; Data are expressed as mean  $\pm$  SEM (n = 2-6) and analyzed using one-way ANOVA with Bonferroni's comparison test. Bars with different letters represent statistically significant differences. *n.s.* represents no significance,  $*p < 0.05$ .



## SubQ



## BAT

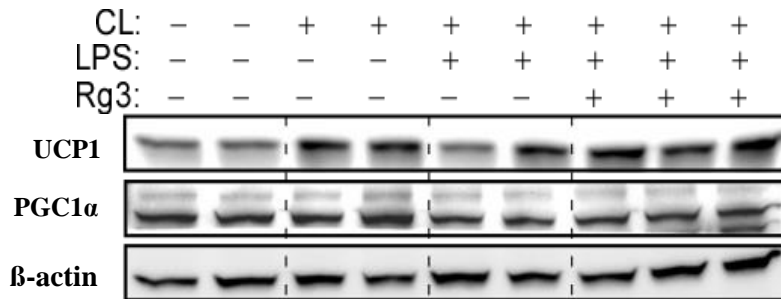


**Fig 18. Effect of Rg3 increased protein expressions by Western blot analysis.**

Immunoblots of UCP1, and OXPHOS complex I-V in SubQ fat; Immunoblots of UCP1, and PGC1 $\alpha$  in BAT; Data are expressed as mean  $\pm$  SEM (n = 2-6) and analyzed using one-way ANOVA with Bonferroni's comparison test. Bars with different letters represent statistically significant differences. *n.s.* represents no significance, *\*p* < 0.05.

## BAT

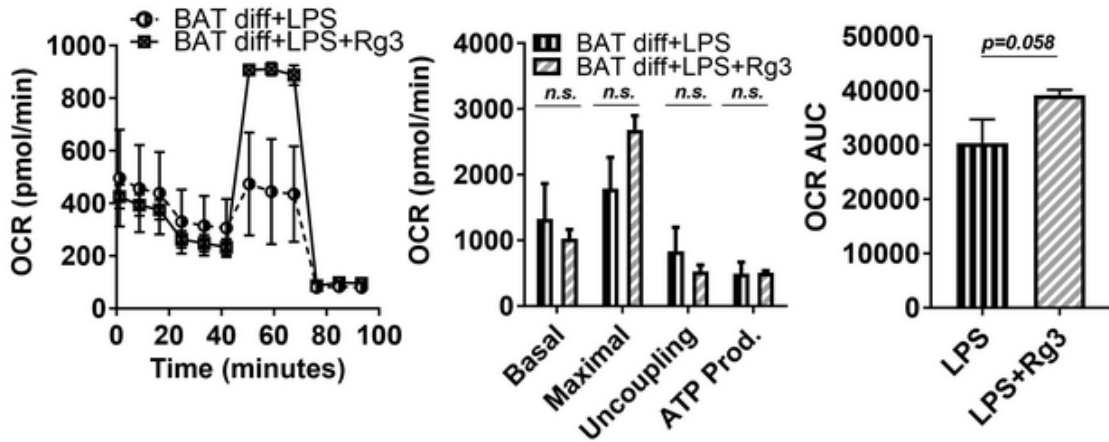


**Fig 19. Rg3 recovers LPS-induced inhibition of browning by upregulation mitochondrial oxygen consumption.**

BAT MSCs were induced to differentiation with or without 60  $\mu$ M of Rg3 for 48 h in the presence of LPS (100 ng/ml) for 72 h.; Data are expressed as mean  $\pm$  SEM (n = 2-6) and analyzed using one-way ANOVA with Bonferroni's comparison test. Bars with different letters represent statistically significant differences. *n.s.* represents no significance, \**p* < 0.05.

#### 4. Discussion

Distinct features of brown and/or beige adipocytes vs. white adipocytes were mitochondrial UCP1 in the inner membranes of mitochondria [7, 35]. By acting to decouple oxidative phosphorylation from ATP generation, UCP1 causes heat to be released from cells [35]. During chronic low-grade inflammation like obesity, BAT, and beige fat-mediated adaptive thermogenesis, which is mediated by thermogenic stimuli, is interrupted by inflammation [8, 9, 36]. Thus, finding the bioactive ingredients activating BAT or beige adipocytes possessing anti-inflammatory properties are promising strategies for obesity management. In this study, we proposed that Rg3 contributes to protecting against LPS-induced inhibition of BAT and beige thermogenesis with the induction of mitochondrial activation. According to our knowledge, this work is the first to document the hitherto underappreciated role of Rg3 on thermogenesis and protective effects on inflammation-induced beige and BAT thermogenesis via mitochondrial activation. Here, we asked two fundamental research questions whether Rg3 i) induces BAT activation, ii) and protects against inflammation-induced inhibition of browning or BAT activation.

In our previous research, we determined the anti-adipogenic properties of Rg3 and Rg3-enriched Red ginseng extract (RGE). RGE significantly reduced adipogenesis, evidenced by ORO and adipogenic gene and protein expressions in 3T3-L1 adipocytes. Although the content of Rg3 in RGE was second most high among ginsenosides (Rb1 >Rg3 >Rg2>Rg1 ~ Re ~ Rb2>Rh1>Rg6>Rh2 in RGE), which is around 0.26 mg/g in RGE, but our group decide to use Rg3 as a key molecule because higher bioavailability than other ginsenosides with strong pharmacological activities [32]. Regarding bioavailability, the absorption rate of Rb1 is very low (around 0.64-1% [37]) due to sugar molecules attached to the carbon skeleton [38]. Although most ginsenosides do not reach the intended biological system when administered orally, the bioavailability of Rg3 is higher than Rb1, which is around 2.63% [38]. Several reports

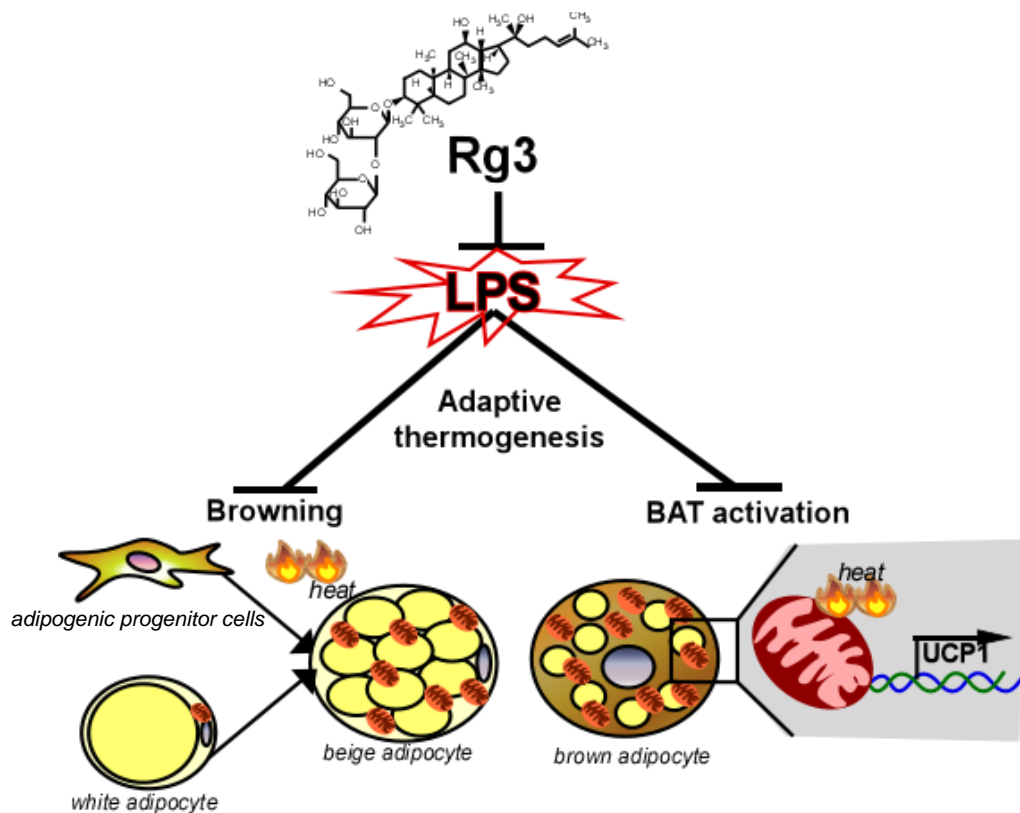
demonstrated that Rg3 had anti-adipogenic effects in adipocytes [22, 23, 39]. In our study, Rg3 treatment reduced the early and late phases of adipogenesis with upregulation of fatty acid oxidation and maximal OCR. We expected that Rg3 treatment (2.5 mg/kg BW) reduced BW or adipose tissue remodeling in animal experiments. With our disappointments, Rg3 treatment for 8 weeks did not alter obesogenic parameters, but Rg3 significantly reduced total cholesterol levels in plasma with lower fasting glucose level. The strong anti-adipogenic/lipogenic effects of Rg3 in cell models, but Rg3 did not have significant effects in an animal model. It indicated the low bioavailability of ginsenosides, although its absorption rate is higher than Rb1. Thus, the manufacturing and/or processing strategy [40] to enhance bioavailability and bioconversion of Rg3 is required for future study.

Recent evidence demonstrated that Rg3 improves mitochondrial population quality and myotube function via mitochondrial functions which mimic exercise training [41, 42]. Given that Rg3 has anti-adipogenic properties with increased mitochondrial functions, we assumed that Rg3 could enhance that mitochondrial-rich beige or BAT activation. Kim et al. Recently addressed that Rg3 treatment (40  $\mu$ M) in mature adipocytes induced browning-related and beige fat specific genes. They also mentioned that AMPK is required for Rg3-mediated browning effects [26]. Mu et al. demonstrated that Rg3 (10 mg/kg BW) via i.p. injection for 8 weeks significantly improved obesogenic parameters such as BW, BWG, lipid profiles, and adipocyte hypertrophy. They also have found that Rg3 can increase the mRNA and protein expression levels of *Ppar $\gamma$* , *Pgc1 $\alpha$* , *Prdm16*, and *Ucp1* in the adipose tissues of obese mice, which indicates adipocyte browning effects of the Rg3 in animals [25]. In our study, Rg3 treatment induced BAT activation via UCP1 upregulation and mitochondrial OCR (Fig.1-3). Although we established beige adipocytes by treatment with cAMP, Rg3 did not significantly upregulate browning features both in 3T3-L1 and SubQ MSCs during adipogenesis (Fig. 4,5). Thus, we turned our gear to investigate the protective role of Rg3 on inflammation-induced inhibition of browning. Recently, it has been reported that

apigenin [43], and *p*-coumaric acid [34] induce adipocyte browning against inflammation. Okla et al. demonstrated that apigenin reversed IL-1 $\beta$  -induced suppression of adipocyte browning via cyclooxygenase (COX2)/ Prostaglandin E2 (PGE2) signaling pathways in human adipocytes [43]. Seo et al. Investigated that *p*-coumaric acid was recovered adipocyte browning against LPS stimulation in adipocytes [34]. The mode of action in anti-inflammation by Rg3 was reported in several cells and animal models, such as TNF $\alpha$ -induced chondrocytes damage [44], allergic airway [45], cisplatin-induced renal toxicity [46], and acetaminophen-induced hepatic inflammation [47]. In our study, the BAT/beige fat activation was accompanied by mitochondrial activation and enhancement of OCR measured by a seahorse analyzer (Fig 1,2, Fig 19). Based on its bioenergetic properties and high amount of antioxidant enzymes in mitochondria, it is presumably assumed that the ROS defense system in mitochondria might reduce inflammation during adaptive thermogenesis [48]. In accordance with our study, Xing et al. Reported that Rg3 attenuated sepsis-induced injury in the liver with mitochondrial biogenesis [49]. Rg3 treatment can inhibit mitochondrial dysfunction via increasing the protein expression of mitochondrial biogenesis-related transcription factors in human primary hepatocytes. Lee et al. demonstrated that Rg3 treatment in atrophic myotubes suppresses mitochondrial reactive oxygen species production via enhancing the activity and expression of PGC1 $\alpha$  [50]. It is still unclear what specific steps of pathways during mitochondrial activation are involved in BAT/beige fat-mediated adaptive thermogenesis against LPS-induced inflammation, but we might guess that PGC1 $\alpha$  or AMPK pathways which many researchers were pointed out, involved in these processes. Thus, further studies are warranted to unravel this issue.

## 5. Conclusion

In conclusion, the present study determined that Rg3 impedes lipid accumulation in adipocytes by augmentation of mitochondrial fatty acid oxidation. Rg3 also activates BAT recruitment in BAT MSCs during brown adipogenesis but not beige adipogenesis. However, Rg3 significantly reverses the inflammation-induced inhibition of BAT and/or beige fat thermogenesis *in vitro* and *in vivo* models induced by cAMP or CL via mitochondrial activation. 2.5 mg/kg BW of Rg3 is a relatively small concentration compared to other experimental conditions [25, 46-48], but still, it is hard to achieve in human physiology. Thus, the clinical relevance and determining the efficacy of Rg3 supplementation should be conducted with caution. Nevertheless, we believe that these discoveries support the potential benefit of Rg3 as a novel brown/beige adipogenic agent to combat inflammation-induced obesity in future clinical studies.



## 6. References

- [1] K.E. Wellen, G.S. Hotamisligil, Obesity-induced inflammatory changes in adipose tissue, *J Clin Invest* 112(12) (2003) 1785-8.
- [2] B.E. Wisse, The inflammatory syndrome: the role of adipose tissue cytokines in metabolic disorders linked to obesity, *J Am Soc Nephrol* 15(11) (2004) 2792-800.
- [3] E.E. Kershaw, J.S. Flier, Adipose tissue as an endocrine organ, *J Clin Endocrinol Metab* 89(6) (2004) 2548-56.
- [4] H.S. Schipper, B. Prakken, E. Kalkhoven, M. Boes, Adipose tissue-resident immune cells: key players in immunometabolism, *Trends Endocrinol Metab* 23(8) (2012) 407-15.
- [5] W.D. van Marken Lichtenbelt, J.W. Vanhommerig, N.M. Smulders, J.M. Drossaerts, G.J. Kemerink, N.D. Bouvy, P. Schrauwen, G.J. Teule, Cold-activated brown adipose tissue in healthy men, *N Engl J Med* 360(15) (2009) 1500-8.
- [6] A.M. Cypess, S. Lehman, G. Williams, I. Tal, D. Rodman, A.B. Goldfine, F.C. Kuo, E.L. Palmer, Y.H. Tseng, A. Doria, G.M. Kolodny, C.R. Kahn, Identification and importance of brown adipose tissue in adult humans, *N Engl J Med* 360(15) (2009) 1509-17.
- [7] K. Ikeda, P. Maretich, S. Kajimura, The Common and Distinct Features of Brown and Beige Adipocytes, *Trends Endocrinol Metab* 29(3) (2018) 191-200.
- [8] M. Okla, W. Wang, I. Kang, A. Pashaj, T. Carr, S. Chung, Activation of Toll-like receptor 4 (TLR4) attenuates adaptive thermogenesis via endoplasmic reticulum stress, *J Biol Chem* 290(44) (2015) 26476-90.
- [9] M. Okla, W. Zaher, M. Alfayez, S. Chung, Inhibitory Effects of Toll-Like Receptor 4, NLRP3 Inflammasome, and Interleukin-1beta on White Adipocyte Browning, *Inflammation* 41(2) (2018) 626-642.

- [10] G.H. Jiang, Z.G. Wu, K. Ameer, S.J. Li, K. Ramachandriah, Particle size of ginseng (Panax ginseng Meyer) insoluble dietary fiber and its effect on physicochemical properties and antioxidant activities, *Appl Biol Chem* 63(1) (2020).
- [11] H. Wang, F. Xu, X. Wang, W.S. Kwon, D.C. Yang, Molecular discrimination of Panax ginseng cultivar K-1 using pathogenesis-related protein 5 gene, *J Ginseng Res* 43(3) (2019) 482-487.
- [12] W.Y. Kim, J.M. Kim, S.B. Han, S.K. Lee, N.D. Kim, M.K. Park, C.K. Kim, J.H. Park, Steaming of ginseng at high temperature enhances biological activity, *J Nat Prod* 63(12) (2000) 1702-4.
- [13] C.Z. Wang, B. Zhang, W.X. Song, A. Wang, M. Ni, X. Luo, H.H. Aung, J.T. Xie, R. Tong, T.C. He, C.S. Yuan, Steamed American ginseng berry: ginsenoside analyses and anticancer activities, *J Agric Food Chem* 54(26) (2006) 9936-42.
- [14] J. Lee, H. Han, X. Yuan, E. Park, J. Lee, J.H. Kim, A rapid, simultaneous and quantitative analysis of 26 ginsenosides in white and red Panax ginseng using LC-MS/MS, *Appl Biol Chem* 64(1) (2021).
- [15] X.D. Yang, Y.Y. Yang, D.S. Ouyang, G.P. Yang, A review of biotransformation and pharmacology of ginsenoside compound K, *Fitoterapia* 100 (2015) 208-20.
- [16] L.W. Qi, C.Z. Wang, C.S. Yuan, American ginseng: potential structure-function relationship in cancer chemoprevention, *Biochem Pharmacol* 80(7) (2010) 947-54.
- [17] K.C. Shin, D.K. Oh, Classification of glycosidases that hydrolyze the specific positions and types of sugar moieties in ginsenosides, *Crit Rev Biotechnol* 36(6) (2016) 1036-1049.
- [18] D.S. Im, Pro-Resolving Effect of Ginsenosides as an Anti-Inflammatory Mechanism of Panax ginseng, *Biomolecules* 10(3) (2020).



- [19] X.J. Chen, X.J. Zhang, Y.M. Shui, J.B. Wan, J.L. Gao, Anticancer Activities of Protopanaxadiol- and Protopanaxatriol-Type Ginsenosides and Their Metabolites, *Evid-Based Compl Alt* 2016 (2016).
- [20] S. Junmin, L. Hongxiang, L. Zhen, Y. Chao, W. Chaojie, Ginsenoside Rg3 inhibits colon cancer cell migration by suppressing nuclear factor kappa B activity, *J Tradit Chin Med* 35(4) (2015) 440-4.
- [21] M. Riaz, N.U. Rahman, M. Zia-Ul-Haq, H.Z.E. Jaffar, R. Manea, Ginseng: A dietary supplement as immune-modulator in various diseases, *Trends Food Sci Tech* 83 (2019) 12-30.
- [22] J.T. Hwang, M.S. Lee, H.J. Kim, M.J. Sung, H.Y. Kim, M.S. Kim, D.Y. Kwon, Antiobesity effect of ginsenoside Rg3 involves the AMPK and PPAR-gamma signal pathways, *Phytother Res* 23(2) (2009) 262-6.
- [23] L. Zhang, L. Zhang, X. Wang, H. Si, Anti-adipogenic Effects and Mechanisms of Ginsenoside Rg3 in Pre-adipocytes and Obese Mice, *Front Pharmacol* 8 (2017) 113.
- [24] O.H. Lee, H.H. Lee, J.H. Kim, B.Y. Lee, Effect of ginsenosides Rg3 and Re on glucose transport in mature 3T3-L1 adipocytes, *Phytother Res* 25(5) (2011) 768-73.
- [25] Q. Mu, J. Zuo, D. Zhao, X. Zhou, J. Hua, Y. Bai, F. Mo, X. Fang, M. Fu, S. Gao, Ginsenoside rg3 reduces body weight by regulating fat content and browning in obese mice, *Journal of Traditional Chinese Medical Sciences* 8(1) (2021) 65-71.
- [26] K. Kim, K.H. Nam, S.A. Yi, J.W. Park, J.W. Han, J. Lee, Ginsenoside Rg3 Induces Browning of 3T3-L1 Adipocytes by Activating AMPK Signaling, *Nutrients* 12(2) (2020).
- [27] H.J. Park, S.M. Jo, S.H. Seo, M. Lee, Y. Lee, I. Kang, Anti-Inflammatory Potential of Cultured Ginseng Roots Extract in Lipopolysaccharide-Stimulated Mouse Macrophages and Adipocytes, *Int J Environ Res Public Health* 17(13) (2020).
- [28] A. Bartelt, O.T. Bruns, R. Reimer, H. Hohenberg, H. Ittrich, K. Peldschus, M.G. Kaul, U.I. Tromsdorf, H. Weller, C. Waurisch, A. Eychmuller, P.L. Gordts, F. Rinninger, K. Bruegelmann,

- B. Freund, P. Nielsen, M. Merkel, J. Heeren, Brown adipose tissue activity controls triglyceride clearance, *Nat Med* 17(2) (2011) 200-5.
- [29] I. Kang, J.C. Espin, T.P. Carr, F.A. Tomas-Barberan, S. Chung, Raspberry seed flour attenuates high-sucrose diet-mediated hepatic stress and adipose tissue inflammation, *J Nutr Biochem* 32 (2016) 64-72.
- [30] S.H. Seo, S.M. Jo, J. Kim, M. Lee, Y. Lee, I. Kang, Peanut Sprout Extracts Attenuate Triglyceride Accumulation by Promoting Mitochondrial Fatty Acid Oxidation in Adipocytes, *Int J Mol Sci* 20(5) (2019).
- [31] I. Kang, Y. Kim, F.A. Tomas-Barberan, J.C. Espin, S. Chung, Urolithin A, C, and D, but not iso-urolithin A and urolithin B, attenuate triglyceride accumulation in human cultures of adipocytes and hepatocytes, *Mol Nutr Food Res* 60(5) (2016) 1129-38.
- [32] J. Zhao, C. Su, C. Yang, M. Liu, L. Tang, W. Su, Z. Liu, Determination of ginsenosides Rb1, Rb2, and Rb3 in rat plasma by a rapid and sensitive liquid chromatography tandem mass spectrometry method: Application in a pharmacokinetic study, *J Pharm Biomed Anal* 64-65 (2012) 94-7.
- [33] M. Han, X. Sha, Y. Wu, X. Fang, Oral absorption of ginsenoside Rb1 using in vitro and in vivo models, *Planta Med* 72(5) (2006) 398-404.
- [34] S.H. Seo, S.-M. Jo, T.T.M. Truong, G. Zhang, D.-S. Kim, M. Lee, Y. Lee, I. Kang, Peanut sprout rich in p-coumaric acid ameliorates obesity and lipopolysaccharide-induced inflammation and the inhibition of browning in adipocytes via mitochondrial activation, *Food & Function* (2021).
- [35] B. Cannon, J. Nedergaard, Brown adipose tissue: function and physiological significance, *Physiol Rev* 84(1) (2004) 277-359.

- [36] M. Alcala, M. Calderon-Dominguez, E. Bustos, P. Ramos, N. Casals, D. Serra, M. Viana, L. Herrero, Increased inflammation, oxidative stress and mitochondrial respiration in brown adipose tissue from obese mice, *Sci Rep* 7(1) (2017) 16082.
- [37] D.H. Kim, Chemical Diversity of *Panax ginseng*, *Panax quinquefolium*, and *Panax notoginseng*, *J Ginseng Res* 36(1) (2012) 1-15.
- [38] F. Zheng, M.Y. Zhang, Y.X. Wu, Y.Z. Wang, F.T. Li, M.X. Han, Y.L. Dai, H. Yue, Biotransformation of Ginsenosides (Rb1 , Rb2 , Rb3 , Rc) in Human Intestinal Bacteria and Its Effect on Intestinal Flora, *Chem Biodivers* 18(12) (2021) e2100296.
- [39] J.B. Lee, S.J. Yoon, S.H. Lee, M.S. Lee, H. Jung, T.D. Kim, S.R. Yoon, I. Choi, I.S. Kim, S.W. Chung, H.G. Lee, J.K. Min, Y.J. Park, Ginsenoside Rg3 ameliorated HFD-induced hepatic steatosis through downregulation of STAT5-PPARgamma, *J Endocrinol* 235(3) (2017) 223-235.
- [40] Y.J. Park, U. Hwang, S. Park, S. Sim, S. Jeong, M. Park, M. Kang, Y. Lee, Y. Song, H. Park, H.J. Suh, Optimal bioconversion for compound K production from red ginseng root (CA Mayer) by sequential enzymatic hydrolysis and its characteristics, *Appl Biol Chem* 64(1) (2021).
- [41] M. Sun, C. Huang, C. Wang, J. Zheng, P. Zhang, Y. Xu, H. Chen, W. Shen, Ginsenoside Rg3 improves cardiac mitochondrial population quality: mimetic exercise training, *Biochem Biophys Res Commun* 441(1) (2013) 169-74.
- [42] S.J. Lee, J.H. Bae, H. Lee, H. Lee, J. Park, J.S. Kang, G.U. Bae, Ginsenoside Rg3 upregulates myotube formation and mitochondrial function, thereby protecting myotube atrophy induced by tumor necrosis factor-alpha, *J Ethnopharmacol* 242 (2019) 112054.
- [43] M. Okla, J.O. Al Madani, S. Chung, M. Alfayez, Apigenin Reverses Interleukin-1beta-Induced Suppression of Adipocyte Browning via COX2/PGE2 Signaling Pathway in Human Adipocytes, *Mol Nutr Food Res* 64(1) (2020) e1900925.

- [44] C.H. Ma, W.C. Chou, C.H. Wu, I.M. Jou, Y.K. Tu, P.L. Hsieh, K.L. Tsai, Ginsenoside Rg3 Attenuates TNF-alpha-Induced Damage in Chondrocytes through Regulating SIRT1-Mediated Anti-Apoptotic and Anti-Inflammatory Mechanisms, *Antioxidants (Basel)* 10(12) (2021).
- [45] W.C. Huang, T.H. Huang, K.W. Yeh, Y.L. Chen, S.C. Shen, C.J. Liou, Ginsenoside Rg3 ameliorates allergic airway inflammation and oxidative stress in mice, *J Ginseng Res* 45(6) (2021) 654-664.
- [46] J.J. Zhang, Y.D. Zhou, Y.B. Liu, J.Q. Wang, K.K. Li, X.J. Gong, X.H. Lin, Y.P. Wang, Z. Wang, W. Li, Protective Effect of 20(R)-Ginsenoside Rg3 Against Cisplatin-Induced Renal Toxicity via PI3K/AKT and NF-[Formula: see text]B Signaling Pathways Based on the Premise of Ensuring Anticancer Effect, *Am J Chin Med* 49(7) (2021) 1739-1756.
- [47] Y. Gao, J. Yan, J. Li, X. Li, S. Yang, N. Chen, L. Li, L. Zhang, Ginsenoside Rg3 ameliorates acetaminophen-induced hepatotoxicity by suppressing inflammation and oxidative stress, *J Pharm Pharmacol* 73(3) (2021) 322-331.
- [48] R.J. Mailloux, Mitochondrial Antioxidants and the Maintenance of Cellular Hydrogen Peroxide Levels, *Oxid Med Cell Longev* 2018 (2018) 7857251.
- [49] W. Xing, L. Yang, Y. Peng, Q. Wang, M. Gao, M. Yang, X. Xiao, Ginsenoside Rg3 attenuates sepsis-induced injury and mitochondrial dysfunction in liver via AMPK-mediated autophagy flux, *Biosci Rep* 37(4) (2017).
- [50] S.J. Lee, M. Im, S.K. Park, J.Y. Kim, E.Y. So, O.D. Liang, J.S. Kang, G.U. Bae, BST204, a Rg3 and Rh2 Enriched Ginseng Extract, Upregulates Myotube Formation and Mitochondrial Function in TNF-alpha-Induced Atrophic Myotubes, *Am J Chin Med* 48(3) (2020) 631-650.

## Supplement Table

**Table1. Dietary composition of high-fat (HF)**

<b>Ingredients</b>	<b>LF</b>	<b>HF</b>
	g/kg	g/kg
Casein	200	200
L-Cysteine	3	3
Sucrose	0	69
Corn starch	600	0
Maltodextrin 10	50	125
Lard	10	245
Cholesterol	0	2
Soybean oil	39	39
Cellulose	50	50
Mineral mix	35	35
Calcium phosphate	4	4
Vitamin mix	10	10
Choline bitartrate	2	2
<b>Total</b>	<b>1003</b>	<b>784</b>
	kcal (%)	kcal (%)
Carbohydrate	67.8	19.8
Protein	20.9	19.3
Fat	11.3	60.8

**Table 2. Primer sequences for real-time PCR**

<b>Gene</b>	<b>Forward</b>	<b>Reverse</b>
mUCP1	AGGCTTCCAGTACCATTAGGT	CTGAGTGAGGCAAAGCTGATTT
mPGC1 $\alpha$	CCCTGCCATTGTTAAGACC	TGCTGCTGTTCTGTTTTTC
mF4/80	CTTTGGCTATGGGCTTCCAGTC	GCAAGGAGGACAGAGTTTATCGTG
mMcp1	AGGTCCCTGTCATGCTTCTG	GCTGCTGGTGATCCTCTTGT
mIL-1 $\beta$	AAATACCTGTGGCCTTGGGC	CTTGGGATCCACACTCTCCAG
mCidea	TGCTCTTCTGTATCGCCAGT	GCCGTGTTAAGGAATCTGCTG
HPRT	TTGCTCGAGATGTCATGAAGGA	AGCAGGTCAGCAAAGAACTTATAGC
m36B4	GGATCTGCTGCATCTGCTTG	GGCGACCTGGAAGTCCAACCT